

How to Cite:

Saju, B., & Rajesh, R. (2022). Denoising and contrast enhancement of normal eye images and slit lamp images of cataract using optimized deep learning model. *International Journal of Health Sciences*, 6(S5), 833–852. <https://doi.org/10.53730/ijhs.v6nS5.8764>

Denoising and contrast enhancement of normal eye images and slit lamp images of cataract using optimized deep learning model

Binju Saju

Research scholar, Sr. Assistant Professor, CHRIST (Deemed to be University), New Horizon College of Engineering, Bangalore, Karnataka, INDIA
Email: binju.saju@res.christuniversity.in

Rajesh R

Associate Professor, CHRIST (Deemed to be University)
Email: r.rajesh@christuniversity.in

Abstract---Denoising and contrast enhancement techniques in normal and slit lamp images are challenging in medical analysis. These images are essential in medical analysis for preventing, diagnosing, and monitoring various diseases. For this purpose, the medical images should be clear. Hence, this work proposes an optimized deep learning model to provide denoised and contrast-enhanced images. To begin, the selection of picture quality is merged to identify high-quality normal as well as slit lamp images for subsequent analysis. The picture quality of an image is examined with the model “Blind/Referenceless Image Spatial Quality Evaluator (BRISQUE)”. It yields a low score for pictures of high-quality, an average score for pictures of medium quality, as well as a high score for images of poor quality. Furthermore, normalization-based contrast limited adaptive histogram equalisation (N-CLAHE) is a new algorithm for converting medium- and low-quality images to high-quality images. The images are then pre-processed to remove noise using wiener filtering (WF) with a convolutional neural network (CNN) with adaptive atom search optimization (CNN-AASO). Further, the denoised image is enhanced by Gaussian mixture-based contrast enhancement (GMCE) for contrast enhancement. The overall implementation is carried out on the Matlab tool. The performance metrics like SNR, PSNR, SSIM, and MSE are evaluated for the proposed model and compared with other enhancement techniques.

Keywords---Denoising, Contrast Enhancement, Deep Learning Model, Score Selection.

Introduction

The slit lamp is a device with a high-intensity source of light that is mostly used to diagnose eye-related problems [1]. It can be used to evaluate ocular tissues, including the cornea, iris, eyelid, and conjunctiva. It contains a bio-microscope connected to a high-intensity light source behind a slit cover [2]. The slit lamp photographs are the means of cataract imaging. Slit lamp operator can change the slit and administer the light to illuminate different positions of the eye and enhance the eye visibility of the patient [3]. In hospitals, slit lamp images are utilized by ophthalmologists to detect eye problems in remote places. This will minimize the time and cost of medical experts traveling to rural areas where there is no need to wait for treatment, and they will be able to continue the therapy [4]. The slit lamp images are essential for cataract detection since they ensure brief details about cataract localization. However, the slit lamp images are affected by noise signals [5]. For these reasons, pre-processing techniques of denoising and contrast enhancement for slit lamp images are becoming a point of huge interest. The slit lamp images need to be improved and developed to have a clear and high-resolution image [6].

Image enhancement is a process that mainly focuses on certain aspects of an image, removing or weakening any unnecessary data by specific requirements [7]. Examples of image enhancement are revealing blurred details, adjusting levels, and eliminating noise to highlight features of an image [8]. Colour image enhancement plays a major role in digital image processing [9]. The image enhancement process includes several models that improve the given image's visual appearance and convert the input image into a better form for excellent analysis by machines. Several image enhancement models are used in the existing works. This is because the uneven illumination is very complex to enhance the slit lamp images directly. Histogram equalization (HE) is a popular model used to improve contrast and based on pixel intensity value distribution. However, the image details will be lost when the grey level is reduced [10]. To address this limitation, adaptive HE (AHE) was introduced, in which the mapping is provided for every pixel differently [11]. In homogenous regions, AHE has extensive contrast enhancement. Hence, the model CLAHE [12] [13] is introduced. However, this model may create artificial boundaries in a region with a sudden grey level change. Several filtering techniques are used in the current work. There are three types of denoising models. They are filtering models [14] [15], transform models [16] [17], and statistical models [18]. Recently, deep learning (DL) models have been used for denoising, and they are mainly utilized in image processing because of their effective results and flexible architecture [19] [20]. Hence, this proposed work uses the DL-based model CNN for denoising and GMCE for contrast enhancement.

Motivation

Slit lamp images play a significant part in the detection of eye-related diseases. The primary benefit of the slit lamp is that it permits us to see the retina with both eyes. These slit lamp photographs provide cost-effectiveness and safety treatment. The brief information about cataracts like nuclear cataract, cortical cataract, as well as posterior subcapsular cataracts might be less contrasted.

Hence, the enhancement of slit lamp images generally helps to check disease based on eye-related problems. The slit lamp images are usually of uneven illumination, blurred, and low contrast.

Further, the slit lamp images may be degraded due to noise, and disturbance may occur due to the camera movement. The primary aim of the slit lamp image enhancement is to enhance the contrast and show the retinal vessels clearly. There are many techniques used for denoising and image enhancement. However, these enhancement models may lead to sudden variations in colour levels, image loss, and artificial boundaries. Hence, developing a better denoised and enhancement model for cataract detection is essential. The significant contributions of the proposed work are:

- Introduces a BRISQUE model for providing the score for the slit lamp images.
- Normalization-based contrast-limited adaptive histogram equalization (N-CLAHE) is introduced to improve low and medium quality images into high-quality images.
- Then, the noise is removed using WF with CNN in the pre-processing stage. Furthermore, the AASOs are applied to improve the overall system performance.
- Finally, the Gaussian mixture-based contrast enhancement (GMCE) method is used to improve the denoised image.

The remaining section of the paper is organized as: Section 2 provides the recent related works based on slit lamp images used in eye disease. Section 3 provides the proposed denoised and enhanced image techniques. Section 4 illustrates the results and discussion, and finally, the overall research work will be concluded in the Section 5.

Related Works

Some of the recent related works based on slit lamp image enhancement and classification models are discussed in this section.

Jiang et al. [21] introduced a model LPSs (Lens partition strategies) using Region CNN (R-CNN) and HT (Hough Transform) to improve infantile cataract diagnosis. A total of 1643 slit lamp images were collected for the purpose of evaluating the LPSs performance. The grading and screening were described by adding multicentre images to the training set. Wang et al. [22] used 5,673 slit-lamp images and 400 smartphone images for the analysis. Initially, the slit lamp images were pre-processed and divided into regional and global images. Then the images were split for training, validation, and testing. Finally, Inception V3 was used to classify the slit lamp images. Hu et al. [23] evaluated the classification of slit lamps by ocular images obtained using a smartphone. The model aimed to automatically identify cataract severity based on nuclear region photometric appearance. The integration of support vector machine (SVM) with ShuffleNet was utilized for finding cataract severity. Gu et al. [24] evaluated a hierarchical DL model comprised of multi-task classifiers used to represent several levels of eye disease. Then, the guided loss function was used to learn the fine-grained

features' variability in eye problems. Finally, the model's performance was verified by ten ophthalmologists with 510 outpatients.

Hu et al. [25] introduced a model for grading and automatic cataract detection using slit lamp images. The primary objective of this work was to create a horizontal scanning video lens. Experimentation proved that the computation speed of the model was much faster than an existing model. Hu et al. [26] used slit lamp images to localise the nuclear region using faster R-CNN with ResNet 101. A normal batch balancing model was introduced to alleviate the imbalance data issue to improve the gradient network training. For the experimentation, the data was collected from 157 patients, and the proposed model processed slit lamp images in exactly 0.1s, which was faster than other models. Liu et al. [27] used a DL model CNN for localization and detection of slit lamp photos. Initially, three grading degrees were introduced by three ophthalmologist, and the lens ROI was located automatically. Then, the dataset was fed to CNN to extract high-level features and prove it's been achieved by quantitative and qualitative analysis.

Proposed Methodology

This section provides an overview of the suggested technique, which is divided into two primary stages. They eliminate noise and contrast enhancement when applied for cataract detection using slit lamp images. This process is considered a challenging process. Generally, in the denoising process, specific details will be lost. This may affect the performance of the model in segmentation and classification. Furthermore, it is also complicated to overcome contrast enhancement while minimizing the noise in uniform regions. The proposed model uses a hybrid model for the image denosing and enhancement process to address such limitations.

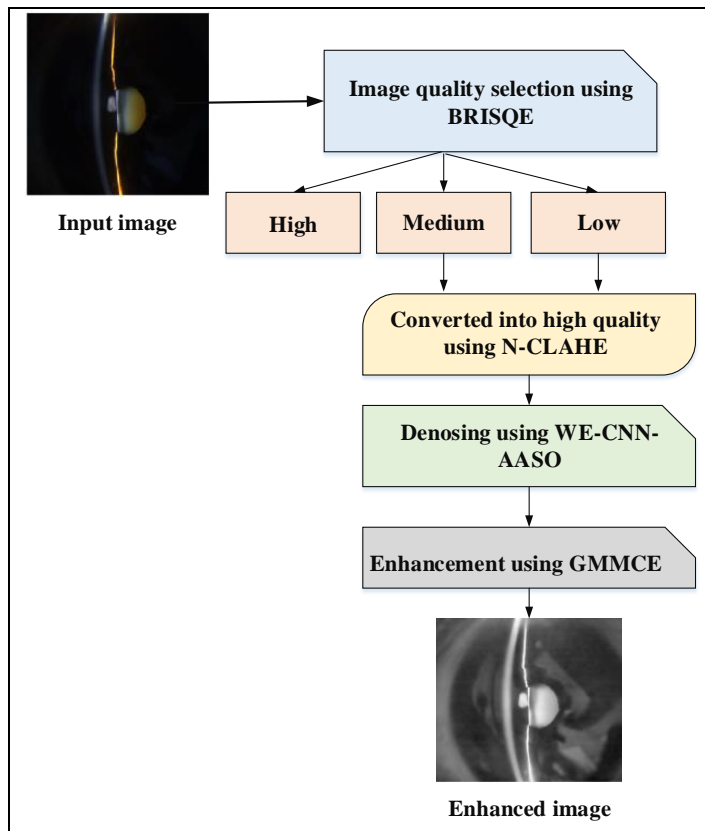


Figure 1. Framework of the proposed denoised and enhancement model

Figure 1 depicts the overall workflow of the proposed denoised and enhancement model. Initially, the score is calculated using the BRISQUE model for selecting the image quality. Then, using this score, only high-quality images will be selected. Further, to improve the number of good images, the poor and medium-quality images are converted into high-quality using N-CLAHE. Then the good images are pre-processed by WF-CNN-AASO, and the denoised image is enhanced by the technique GMCE. The overall methods used in the proposed work are explained in the below sections.

Image Quality Selection Using BRISQUE

In this work, the quality of the image is selected using the BRISQUE score. This method utilizes a spatial technique. Initially, local normalized luminance is also called MSCN (Mean subtracted contrast normalized), and it is computed by:

$$M(p, q) = \frac{\overset{\textcircled{R}}{M}(p, q) - m(p, q)}{s(p, q) + D} \quad (1)$$

where $\vec{M}(p, q)$ is an intensity image, $\mu(p, q)$ as well as $\sigma(p, q)$ are the local mean and variance and $D = 1$. The value of $\mu(p, q)$ as well as $\sigma(p, q)$ is computed by the following expressions.

$$m(p, q) = \mathring{a}_{s=-s}^S \mathring{a}_{u=-U}^U W_{s,u} I_{s,u}^{\textcircled{R}}(p, q) \quad (2)$$

$$s(p, q) = \sqrt{\mathring{a}_{s=-s}^S \mathring{a}_{u=-U}^U W_{s,u} I_{s,u}^{\textcircled{R}}(p, q) - m(p, q)} \quad (3)$$

where $W_{s,u}$ is a 2D circularly symmetric Gaussian weighted term. Finally, the score is calculated, and let us consider [29] when the score is 0–35, then the image is regarded as good quality. When the score is 36–50, the image is considered medium quality, and when the score is 51–100, the image is regarded as poor quality. Initially, there are 425 normal and 181 slit lamp images. From these images, 315 (normal) and 54 (slit lamp) good quality images are obtained.

N-Clahe

Further, to increase the number of high-quality images, the N-ClaHE model is used. N-CLAHE is an integration of normalization and CLAHE. This model increases the low and medium-quality images into better quality images. This process undergoes two phases. Initially, intensity correlation is computed using a log normalization term that controls the intensity image contrast. Then the CLAHE model is used to enhance the local contrast and texture of images. Normalization is a method used to vary the pixel intensity range values, and it is represented as:

$$Q_N = \log \frac{\mathring{a} Q_b}{\mathring{a} Q_R} \quad (4)$$

where Q_N is a normalized image, Q_b is an image without the object and Q_R is a typical image.

Then, the CLAHE is performed by limiting the histogram amplification in an image and then clipping the histogram amplification. CLAHE splits the image into small, overlapped tiles to achieve this. The enhancement of contrast is then applied to each tile using HE. The clip limit is utilized to overcome the noise amplification issues. Hence, every tile is increased, hence the processed histogram segment nearly matches the histogram indicated using distribution functions like Gaussian, Rayleigh, and uniform. Before calculating the CDF (Cumulative Distribution Function), the histogram will be clipped at a particular range to minimize the noise amplification. CLAHE is based on two major factors: clip limit and tile size. The enhanced image quality is managed by these factors. The Rayleigh distribution is commonly used to clip histograms and is denoted as:

$$z(j) = z_{\min} + \sqrt{2(l^2) \ln \frac{1}{1-s(j)}} \quad (5)$$

where z_{\min} is a lower limit of pixel value, λ is Rayleigh's scaling parameter and $s(j)$ is cumulative probability that is used for creating transfer function. When the λ value is increased, there will be more contrast enhancement in an image. Further, the value of saturation and noise level amplification also increases. Therefore, while applying the N-CLAHE filter, the number of good pictures increases from 315 to 401 for normal images and from 54 to 139 for slit lamp images.

Denoising using WF-CNN-AASO

Once the images are converted into high-quality images, they are pre-processed (denoised) using WF-CNN-AASO. Image denoising is a major method in the field of image processing. It is a method of removing the noise from the noise and managing the key features. Initially, the image is pre-processed by WF. It is a low-pass filter that is provided in several contexts for restoring noise-degraded signals. This filter is based on a statistical model that takes into account the signal as well as noise, a stationary linear stochastic model with well-known spectral features. The filter decreases the difference between the predicted as well as original signals. Let o_r and e_s be the uncorrupted and estimated image, then the error is measured by the following expression:

$$error = EA \left\{ (o_r - e_s)^2 \right\} \quad (6)$$

where $EA\{\cdot\}$ is an expected argument value. Hence, the estimated image is minimized to identify the minimum quadratic error factor. A frequency domain is utilised to achieve this. When the image and noise are uncorrelated, the image and noise have a zero mean, and the levels of intensity in an estimated image are minimized using a linear function. According to that, the minimum error factor is given as:

$$P(x, y) = \frac{D^*(x, y) R(x, y)}{\sqrt{|D(x, y)|^2 + R(x, y)}} C(x, y) \quad (7)$$

where $P(x, y)$ is an estimated image, $D(x, y)$ is a degradation term transform, $C(x, y)$ is degraded image transform and $D^*(x, y)$ is a $D(x, y)$ complex conjugate. The output image obtained by WF is given as an input to CNN. Figure 2 depicts the architecture of denoised CNN-AASO. It comprises of 3 layers. They are convolution (conv) + rectified linear units (ReLU), conv + batch normalization (BN) and conv layer.

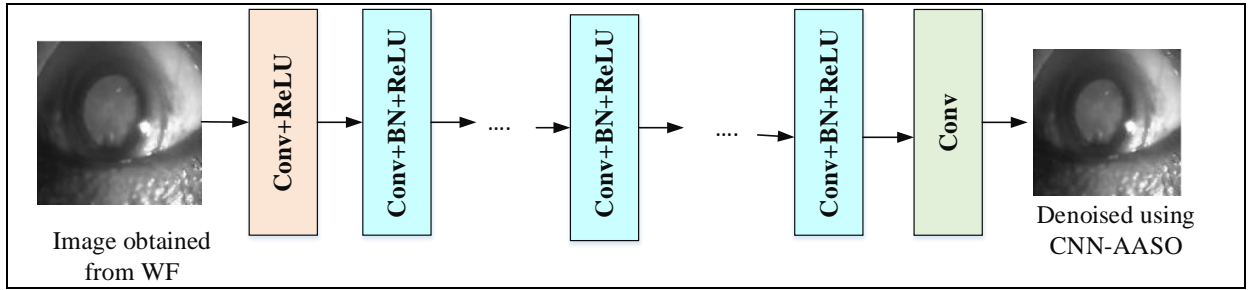


Figure 2. Architecture of denoised CNN-AASO

- (i) The first layer has a 64 filters with a size of $3 \times 3 \times d$ is used for generating 64 feature maps and d is the number of image channels. ($ReLU, \max(0, \cdot)$) is exploited for non-linearity.
- (ii) In second layer to $L-1$, there are 64 filters with a size of $3 \times 3 \times 64$ is utilized and BN is included between ReLU and convolution. The BN is used for alleviating the internal covariate shift effect and to increase the process of training.
- (iii) For the final layer, d filter of size $3 \times 3 \times 64$ is utilized for reconstructing the output. In every layer, zero length padding 1 is included before conv, therefore the dimension of image doesn't vary since it passed via network.

The obtained image in image processing is affected due to degradation term and additive noise and it is expressed as:

$$I'(u, v) = I(u, v) + b(u, v) \quad (8)$$

where $I'(u, v)$, $I(u, v)$ and $b(u, v)$ are the obtained image, original image and additive noise.

Residual mapping is utilized for estimating the noise n . That is $R_e(I') \approx b$. Based on this the original image $I(u, v)$ is expressed as:

$$I(u, v) = I'(u, v) - R_e(I') \quad (9)$$

The loss function which is reduced in the estimation is the average mean square error among the estimated noise and residual image and it is expressed as:

$$L_o(Q) = \frac{1}{2M} \sum_{j=1}^M \|R_e(I'_j; Q) - (I'_j - I_j)\|_S^2 \quad (10)$$

The Equation (10) is used for learning the training parameter Θ . I'_i and I_i are the noise image matrix and ground truth image matrix. M is overall training samples. It is complex to train CNN in the denoising process, and it also suffers from performance saturation. To make the weight of CNN lighter and get a denoised image, the optimization method adaptive atom search optimization is used.

The inspiration for AASO [28] is molecular dynamics, which depicts the matter structure and interconnected atoms. The search is performed using interaction force from constraint forces on pairs of atoms and potential energy. The force of interaction has a repulsion and attraction joining the atoms. When the equilibrium distance is greater than the distance among pair of atoms, then the force of interaction is defined by attraction. When the equilibrium distance is less than the distance between atoms, then the force of interaction is defined by repulsion. The mass of atoms is measured using the fitness value of the present atom population, and it is defined as:

$$M_k(T) = \exp \left[\frac{F_k(T) - F_b(T)}{F_w(T) - F_b(T)} \right] \quad (11)$$

$$m_k(T) = \frac{M_k(T)}{\sum_{l=1}^n M_l(T)} \quad (12)$$

where $M_k(T)$ and $m_k(T)$ are the mass and normalized mass of k^{th} atom. $F_w(T)$ and $F_b(T)$ are the worst and best fitness of entire atoms.

The entire force on the k^{th} atom from the different atoms are given as:

$$F_k^d(T) = \sum_{l=1}^n r_l F_{kl}^d(T) \quad (13)$$

$$F_{kl}^d(T) = -a(T) \left[2(p_{kl}(t))^{13} - (p_{kl}(t))^7 \right] \quad (14)$$

where r_l is a random number and it ranges from [0,1] and $a(T)$ is a depth factor and it is given as:

$$a(T) = h \exp \left[-\frac{T-1}{t} \right] \exp \left[-\frac{20}{t} \right] \quad (15)$$

The force of constraint is given as:

$$C_k^d(T) = g(T)(y_b^d(T) - y_k^d(T)) \quad (16)$$

where $\gamma(T)$ is a Lagrangian multiplier and $y_b^d(T)$ is a best atom position.

During the entire iterations, the resulting force of k^{th} atom is given as:

$$R_f = F_k^d(T) + C_k^d(T) \quad (17)$$

Based on the Newton's law of motion, k^{th} atom acceleration is expressed as:

$$a_k^d(T) = \frac{F_k^d(T)}{m_k^d(T)} + \frac{C_k^d(T)}{m_k^d(T)} \quad (18)$$

Finally, the position and velocity of the k^{th} atom at time $T+1$ is given as:

$$v_k^d(T+1) = r_k^d v_k^d(T) + a_k^d(T) \quad (19)$$

$$p_k^d(T+1) = p_k^d(T) + v_k^d(T+1) \quad (20)$$

Even though the ASO has better optimization performance, the exploitation and exploration behaviours are poor. Hence, an additional force must be required to improve the atom speed to improve these two behaviours. Therefore, the velocity and position of the atoms are updated by the following equation:

$$v_k^d(T+1) = r_k^d v_k^d(T) \cos(T\pi) + a_k^d(T) \sin(T\pi) \quad (19)$$

where $\cos(T\pi)$ and $\sin(T\pi)$ are the accelerating weights which improves the exploitation and exploration behaviour. Hence, the denoised image will be obtained clearly.

Image Enhancement using GMCE

After denoising, the image is enhanced using GMCE. For modelling the image contents, this model employs Gaussian Mixture (GM) of histograms. Every homogenous area in an image has a Gaussian shape structure. It is used to decompose the narrow histogram of less contrasted images into groups of shifted and scaled Gaussians. These Gaussians are partitioned based on the average value and spread out the variance, forming a global histogram. Hence, low-contrast images have a narrow histogram, and when one leaves the necessary means from one another, the contrast of the areas will be increased, and the image's visual quality will also be increased.

Every arbitrary histogram is a weighted sum of l Gaussian that needs to determine 3 vectors of l parameters. They are scaling function ε , mean μ and variance σ^2 . Hence, the GM of histogram is given as:

$$H_{GM}^l(I | s^2, e, m) = \sum_{k=1}^j e_k M(I | s_k^2, m_k) \quad (20)$$

where $M(I | \sigma_k^2, \mu_k)$ is a k^{th} Gaussian probability density function (PDF) having the interval range of $I \in [0, P-1]$. Based on Equation (1), a height of every

Gaussian is scaled using ε_k and it is corresponding to place is filled by the respective region. The variation between the GM and an original is optimized and it is expressed as:

$$\arg \min_{s, e, m} \mathring{\mathbf{a}} \sum_{I=0}^{P-1} H_o(I) - H_{GM}^l(I | s^2, e, m) \quad (21)$$

where H_o is an original image histogram.

For estimating the mean parameter, the GMCE models takes the intensity phase and it is expressed as:

$$m = \arg \max_I \mathring{\mathbf{a}} \sum_{k=0}^{P-1} M(k | I, s_0^2) H_o(k) \quad (22)$$

Then, for estimating the variance boundaries and sub-histogram are considered as inputs. After finding the sub-histogram, the scaling factor is estimated using the following equation.

$$n_s^{t+1}(I) = n_s^t(I) - e \mathring{\mathbf{a}} M(I | m, s_0^2) \quad (22)$$

Finally, the intensity level is assigned as the output for histogram matching factor R for input S_1 .

$$R(S_1) = S_2 \quad (23)$$

The enhancement model of GMCE is carried out completely by providing R for each pixel of low contrast images. Thus, the image is enhanced efficiently by the GMCE model and it can be used for predicting the cataract.

Results and Discussion

The proposed denoising and enhancement are simulated on the MATLAB platform. The robustness of the proposed approach is analysed based on the quality of images. The overall evaluation is carried out on an 8 GB RAM, Intel Core i5 CPU with a 3.0 GHz speed. For implementing the proposed scheme, the simulation tool MATLAB is used.

Dataset Details

The dataset is real-time data collected from the Kerala-based Little Flower Research Centre. The camera captures the slit lamp images. Further, the slit images are collected from normal people and patients affected by cataract. There are 425 normal and 181 slit lamp images available in the dataset. A sample image representation is depicted in Figure 3.

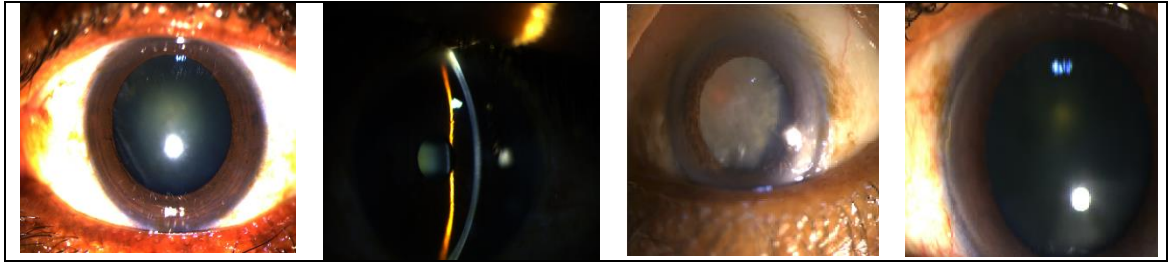


Figure 3. Sample images from the dataset

Performance Measure

Visual quality and image enhancement are regarded as subjective problems. The performance metrics are used to assess the impact of enhancement on normal as well as slit lamp images. Multiple image quality measures are applied for testing the proposed image enhancement model. These metrics are explained below.

Mean Squared Error (MSE): It is the cumulative squared error among the actual and obtained values and it is given as

$$MSE = \frac{1}{m} \sum_{i=1}^n (c_i - d_i)^2 \quad (24)$$

where c_i is the actual image, d_i is the estimated image and m is image size.

Peak Signal to Noise Ratio (PSNR): It is the ratio of maximum intensity in an output image to the value of MSE and it is expressed as:

$$PSNR = 10 \cdot \log_{10} \frac{I_o^{m^2}}{MSE} \quad (25)$$

where $I_o^{m^2}$ is the maximum intensity in an output image.

Structure similarity index (SSIM): This measure is used for comparing the luminance $l(c_i, d_i)$, structure $s(c_i, d_i)$ and contrast $c_o(c_i, d_i)$ of two dissimilar image. It is represented by the below Equation.

$$SSIM = [l(c_i, d_i)], [c_o(c_i, d_i)], [s(c_i, d_i)] \quad (26)$$

Signal to noise ratio (SNR): It is the ratio of noisy image to that of the variation among the original and noisy image and it is expressed as:

$$SNR = \frac{\sum_{j=0}^{M-1} \sum_{k=0}^{N-1} z(j, k)^2}{\sum_{j=0}^{M-1} \sum_{k=0}^{N-1} [y(j, k) - z(j, k)]^2} \quad (27)$$

where $z(j, k)$ is a noisy image and $y(j, k)$ is an original image.

Performance Comparison of Normal Images

This section shows the performance comparison of the normal images. The proposed denoised and enhancement results and the qualitative and numerical results are presented below.

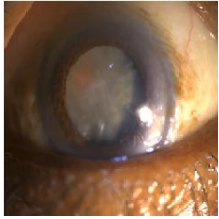
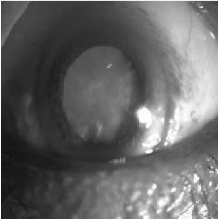
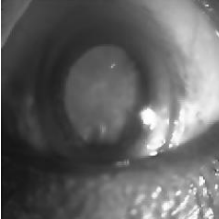
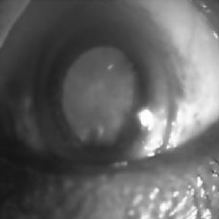
IMAGE 1 (High-quality)				
	Input image	Gray image with score with 25.3	WF-CNN-AASO	GMCE

Figure 4 (a). Qualitative analysis for the high-quality image

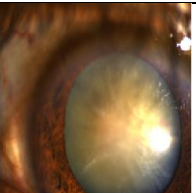
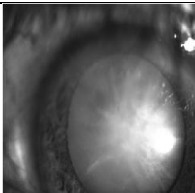
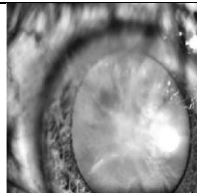
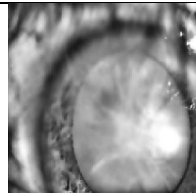
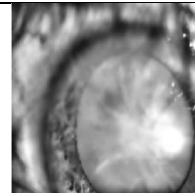

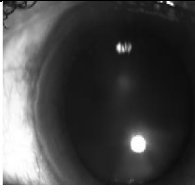
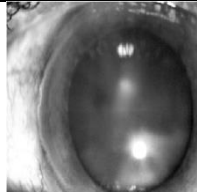
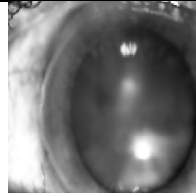
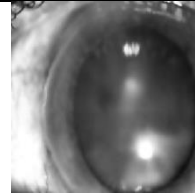
IMAGE 2 (Medium quality)					
	Input image	Gray image with score with 37.7	N-CLAHE image with score 22.8	WF-CNN-AASO	GMCE
IMAGE 3 (Poor quality)					
	Input image	Gray image with score with 48.9	N-CLAHE image with score 24.4	WF-CNN-AASO	GMCE

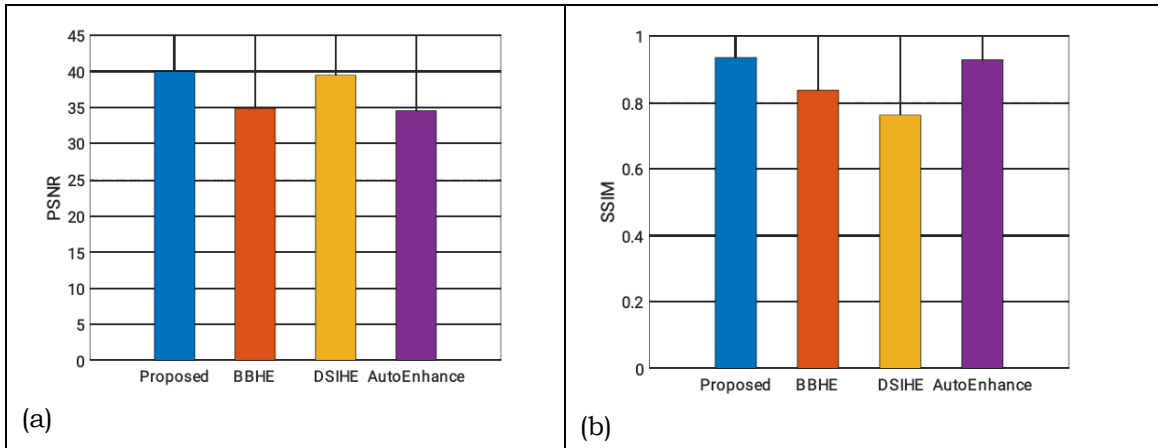
Figure 4(b). Qualitative analysis for the medium and poor quality images

Figure 4 (a) and (b) represent the qualitative analysis for the high-quality image. Initially, the input is converted into a grayscale image. Using the BRISQE score, for this high-quality image value, 25.3 will be obtained. Then the image is denoised using WF-CNN-AASO, and the enhanced image is obtained using GMCE. The image core obtained for medium and high-quality images is 37.7 and 48.9, respectively. Hence, to improve the image score for these two images, the image quality is enhanced by N-CLAHE. So, the image score will be 22.8 and 24.4 for these two images. After this, denoising and contrast enhancement are applied.

Table 1
Performance comparison of the high, medium and low-quality images

Images	Methods	SNR	PSNR	SSIM	MSE
IMAGE 1 (high-quality)	WF-CNN-AASO	82.025	41.954	0.9601	4.1459
	WF-CNN-AASO+GMMCE	83.918	42.505	0.9603	3.6519
IMAGE 2 (Medium quality)	N-CLAHE	19.950	42.954	0.6957	3.2934
	N-CLAHE+WF-CNN-AASO	20.121	43.520	0.7311	2.8908
	N-CLAHE+WF-CNN-AASO+GMMCE	20.187	43.639	0.7304	2.8127
IMAGE 3 (Poor quality)	N-CLAHE	18.519	47.373	0.6512	1.1906
	N-CLAHE+WF-CNN-AASO	18.565	45.796	0.6743	1.7116
	N-CLAHE+WF-CNN-AASO+GMMCE	18.578	48.307	0.6743	1.1218

Table 1 depicts the performance comparison of the high, medium, and low-quality images. When the PSNR value is high, it shows less noise in the image. This indicates that the image quality is high. SSIM is used for preserving the structures and details of the two images. The PSNR and SSIM of the poor quality image are 48.307 and 0.6743, respectively. The denoised and enhancement model depicts the better SNR, SSIM, PSNR, and MSE values for all three images. The proposed technique outperforms the techniques when it is applied individually.



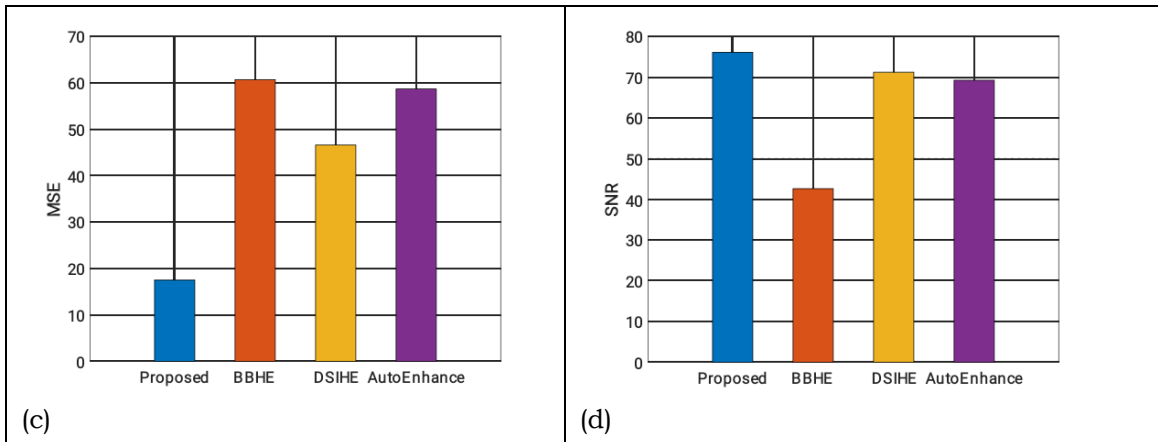


Figure 5. Comparison of image enhancement of various approaches (a) PSNR (b) SSIM (c) MSE, and (d) SNR

Figure 5 represents the comparison of image enhancement of various approaches like BBHE (Brightness Preserving Bi-HE), DSIHE (Dualistic Sub Image-HE), Auto enhancement (AE), and the proposed enhancement model. The graphical representation shows that the proposed enhancement model has achieved better results based on PSNR, SSIM, MSE, and SNR values. Due to recursion, the time complexity was high for the existing enhancement models. So they attained poor results than the proposed WF-CNN-AASO+GMMCE.

Performance Comparison of Slit Lamp Images

This section illustrates the performance comparison of the slit lamp images. The qualitative and quantitative analysis of the proposed denoised and enhancement model (WF-CNN-AASO+GMMCE) is explained briefly.

IMAGE 1 (High-quality)				
	Input image	Gray image with score with 30.4	WF-CNN-AASO	GMCE

Figure 6 (a). Qualitative analysis for the high-quality slit lamp image

IMAGE 2 (Medium quality)					
	Input image	Gray image with score	N-CLAHE image with	WF-CNN-AASO	GMCE


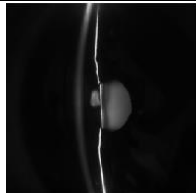
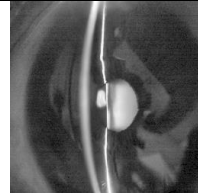
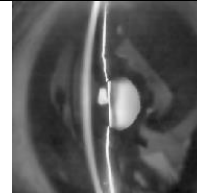
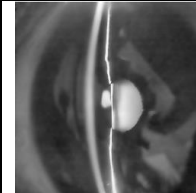
		with 43.2	score 20.5		
IMAGE 3 (Poor quality)					
	Input image	Gray image with score with 53.81	N-CLAHE image with score 25.06	WF-CNN-AASO	GMCE

Figure 6 (b). Qualitative analysis for the medium and poor quality slit lamp images

Figure 6 (a) and (b) represent the qualitative analysis for the high, medium, and low-quality images. With the help of the BRISQE score, the score values are obtained. For this high-quality image, a score value of 30.4 is achieved. The image core achieved for the medium and high-quality images is 43.2 and 53.81, respectively. Hence, to improve the image score, the quality of the image is enhanced by N-CLAHE. Therefore, the image score will be 20.5 and 25.06 for these two images. Finally, denoising and contrast enhancement are applied.

Table 2
SNR, PSNR, SSIM, and MSE comparison of the three quality images

Images	Method	SNR	PSNR	SSIM	MSE
IMAGE 1	N-CLAHE+WF-CNN-AASO	69.7520	38.7017	0.9310	1.7682
	N-CLAHE+WF-CNN-AASO+GMMCE	72.5482	41.9276	0.9712	1.3237
IMAGE 2	N-CLAHE	8.0951	87.2647	0.3626	1.2207e-04
	N-CLAHE+WF-CNN-AASO	10.0861	56.7517	0.3885	0.1374
	N-CLAHE+WF-CNN-AASO+GMMCE	11.0710	58.6063	0.3971	0.0896
IMAGE 3	N-CLAHE	5.5755	95.2956	0.1806	1.5259e-05
	N-CLAHE+WF-CNN-AASO	5.5779	95.2956	0.2172	0
	N-CLAHE+WF-CNN-AASO+GMMCE	6.5779	97.2956	0.2672	0

Table 2 indicates the SNR, PSNR, SSIM, and MSE comparison of the three quality images of the slit lamp images. For image 1, the PSNR of the WF-CNN-AASO+GMMCE is 41.9276, the SNR is 72.5482, the SSIM is 0.9712, and the MSE is 1.3237. The MSE value is very low for the proposed model. This shows that this model has less error and can be efficiently used in cataract detection.

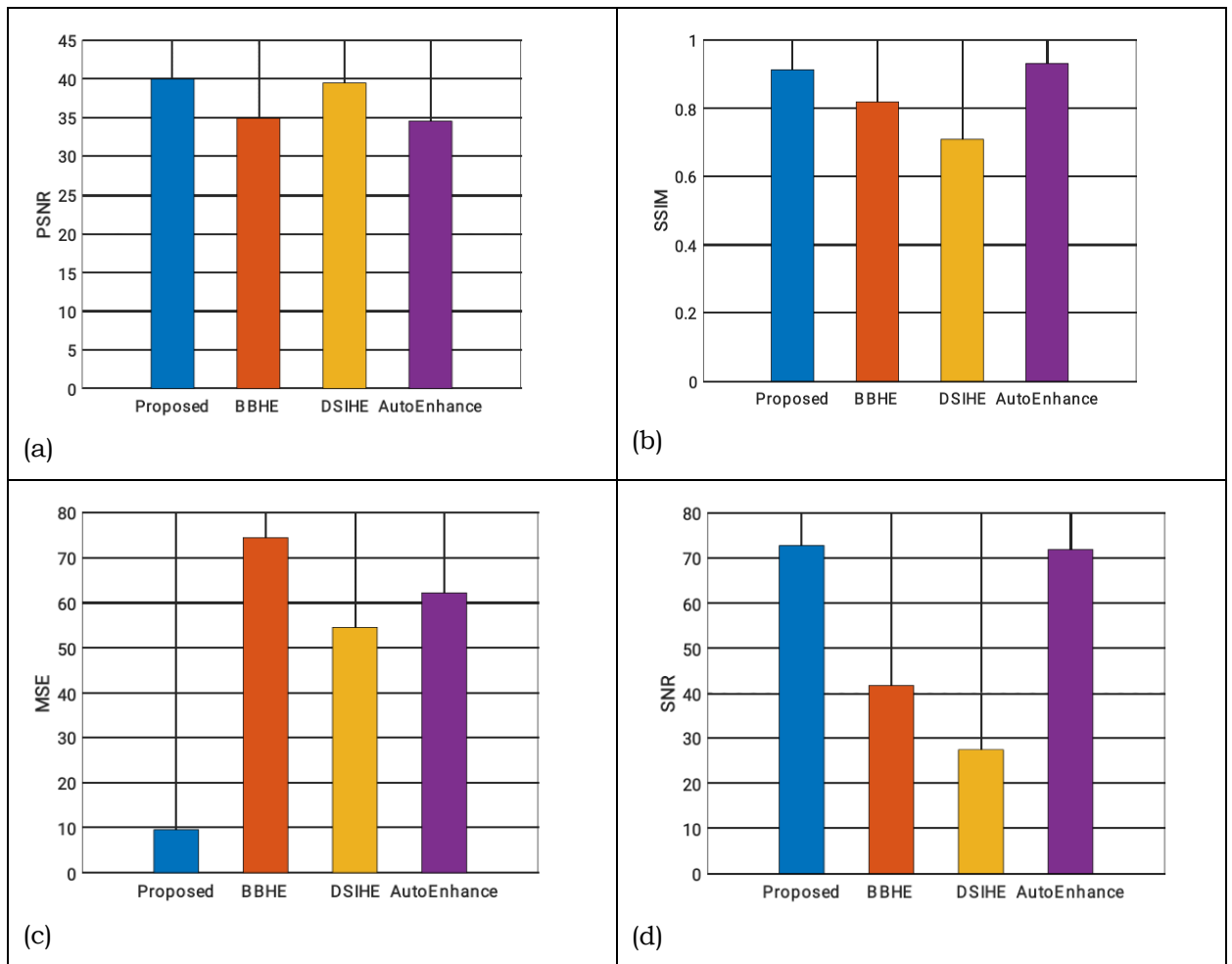


Figure 7. Comparison of image enhancement of various approaches (a) PSNR (b) SSIM (c) MSE, and (d) SNR

Figure 7 shows the comparison of image enhancement of different models, such as BBHE, DSIHE, Auto enhancement (AE), and the proposed WF-CNN-AASO+GMMCE. From the graphical illustration, it is found that the proposed model has achieved better results, that is, PSNR = 40, SSIM = 0.925, MSE = 10, and SNR = 74. This shows that the enhanced image attained with the proposed model preserves the features and is well-structured of the original image.

Conclusion

Denoising and contrast enhancement are the most complex tasks in the pre-processing of slit lamp images, particularly in cataract detection. This paper presents an effective and simple pre-processing model concerning integrating the denoising and contrast enhancement of normal and slit lamp images. Initially, for the image quality selection, the score is selected using the BRISQE score. Then, further improving the low and medium-quality images, N-CLAHE is used. This

will increase the number of good-quality images. Then these images are pre-processed by WF-CNN-AASO.

Further, the denoised image is enhanced using GMCE. The quantitative and qualitative analysis are presented. The robustness of the proposed WF-CNN-AASO+GMMCE is compared with that of the conventional image enhancement techniques based on SNR, SSIM, PSNR, and MSE. The proposed model depicts the higher achievements in all three cases (high, medium, and low). In the future, this enhanced image can be utilized in cataract detection, which will reduce the work of ophthalmologists.

References

- [1] Dutt S, Nagarajan S, Vadivel SS, Baig AU, Savoy FM, GanapathyVM, Dominic M, Sivaraman A, Rao DP. Design and Performance Characterization of a Novel, Smartphone-Based, Portable Digital Slit Lamp for Anterior Segment Screening Using Telemedicine. *Translational Vision Science & Technology*. 2021 Jul 1;10(8):29.
- [2] Lee JS. Slit Lamp Exam. In *Primary Eye Examination 2019* (pp. 101-111). Springer, Singapore.
- [3] GohJH, Lim ZW, Fang X, Anees A, Nusinovici S, Rim TH, Cheng CY, ThamYC. Artificial intelligence for cataract detection and management. *The Asia-Pacific Journal of Ophthalmology*. 2020 Mar 1;9(2):88-95.
- [4] Li JP, Liu H, Ting DS, Jeon S, Chan RP, Kim JE, Sim DA, Thomas PB, Lin H, Chen Y, Sakomoto T. Digital technology, tele-medicine and artificial intelligence in ophthalmology: A global perspective. *Progress in retinal and eye research*. 2021 May 1;82:100900.
- [5] Yazu H, Shimizu E, Okuyama S, Katahira T, Aketa N, Yokoiwa R, Sato Y, Ogawa Y, Fujishima H. Evaluation of nuclear cataract with smartphone-attachable slit-lamp device. *Diagnostics*. 2020 Aug;10(8):576.
- [6] Wan ZakiWM, Abdul Mutalib H, Ramlan LA, Hussain A, Mustapha A. Towards a Connected Mobile Cataract Screening System: A Future Approach. *Journal of Imaging*. 2022 Feb;8(2):41.
- [7] Qi, Y., Yang, Z., Sun, W., Lou, M., Lian, J., Zhao, W., Deng, X. and Ma, Y., 2021. A comprehensive overview of image enhancement techniques. *Archives of Computational Methods in Engineering*, pp.1-25.
- [8] Pourasad Y, Cavallaro F. A novel image processing approach to enhancement and compression of X-ray images. *International Journal of Environmental Research and Public Health*. 2021 Jan;18(13):6724.
- [9] Bansal A, Singh N. Image Enhancement Techniques: A Review. *Asian Journal For Convergence In Technology (AJCT) ISSN-2350-1146*. 2020 Aug 29;6(2):07-11.
- [10] Xie, Y., Ning, L., Wang, M. and Li, C., 2019, October. Image enhancement based on histogram equalization. In *Journal of Physics: Conference Series* (Vol. 1314, No. 1, p. 012161). IOP Publishing.
- [11] Huang, J., Ma, Y., Zhang, Y. and Fan, F., 2017. Infrared image enhancement algorithm based on adaptive histogram segmentation. *Applied optics*, 56(35), pp.9686-9697.
- [12] dos Santos JC, Carrijo GA, de Fátima dos Santos Cardoso C, Ferreira JC, Sousa PM, Patrocínio AC. Fundus image quality enhancement for blood

- vessel detection via a neural network using CLAHE and Wiener filter. *Research on Biomedical Engineering*. 2020 Jun;36(2):107-19.
- [13] Ningsih DR. Improving retinal image quality using the contrast stretching, histogram equalization, and CLAHE methods with median filters. *International Journal of Image, Graphics and Signal Processing*. 2020 Apr 1;10(2):30.
- [14] Rejeesh, M.R. and Thejaswini, P.M.O.T.F., 2020. MOTF: Multi-objective Optimal Trilateral Filtering based partial moving frame algorithm for image denoising. *Multimedia Tools and Applications*, 79(37), pp.28411-28430.
- [15] Ma R, Hu H, Xing S, Li Z. Efficient and fast real-world noisy image denoising by combining pyramid neural network and two-pathway unscented Kalman filter. *IEEE Transactions on Image Processing*. 2020 Jan 20;29:3927-40.
- [16] Lyu Z, Zhang C, Han M. A nonsampledcountourlet transform based CNN for real image denoising. *Signal Processing: Image Communication*. 2020 Mar 1;82:115727.
- [17] Bnou, K., Raghay, S. and Hakim, A., 2020. A wavelet denoising approach based on unsupervised learning model. *EURASIP Journal on Advances in Signal Processing*, 2020(1), pp.1-26.
- [18] Wei K, Fu Y, Huang H. 3-D quasi-recurrent neural network for hyperspectral image denoising. *IEEE transactions on neural networks and learning systems*. 2020 Mar 25;32(1):363-75.
- [19] Tian C, Fei L, Zheng W, Xu Y, Zuo W, Lin CW. Deep learning on image denoising: An overview. *Neural Networks*. 2020 Nov 1;131:251-75.
- [20] Tian, C., Xu, Y. and Zuo, W., 2020. Image denoising using deep CNN with batch renormalization. *Neural Networks*, 121, pp.461-473.
- [21] Jiang, J., Lei, S., Zhu, M., Li, R., Yue, J., Chen, J., Li, Z., Gong, J., Lin, D., Wu, X. and Lin, Z., 2021. Improving the Generalizability of Infantile Cataracts Detection via Deep Learning-Based Lens Partition Strategy and Multicenter Datasets. *Frontiers in Medicine*, 8, p.470.
- [22] Wang L, Chen K, Wen H, Zheng Q, Chen Y, Pu J, Chen W. Feasibility assessment of infectious keratitis depicted on slit-lamp and smartphone photographs using deep learning. *International journal of medical informatics*. 2021 Nov 1;155:104583.
- [23] Hu, S., Wang, X., Wu, H., Luan, X., Qi, P., Lin, Y., He, X. and He, W., 2020. Unified diagnosis framework for automated nuclear cataract grading based on smartphone slit-lamp images. *IEEE Access*, 8, pp.174169-174178.
- [24] Gu H, Guo Y, Gu L, Wei A, Xie S, Ye Z, Xu J, Zhou X, Lu Y, Liu X, Hong J. Deep learning for identifying corneal diseases from ocular surface slit-lamp photographs. *Scientific reports*. 2020 Oct 20;10(1):1-1.
- [25] Hu S, Luan X, Wu H, Wang X, Yan C, Wang J, Liu G, He W. ACCV: automatic classification algorithm of cataract video based on deep learning. *BioMedical Engineering OnLine*. 2021 Dec;20(1):1-7.
- [26] Xu C, Zhu X, He W, Fully Deep Learning for Slit-Lamp Photo Based Nuclear Cataract Grading, *International Conference on Medical Image Computing and Computer-Assisted Intervention*. Springer, Cham. 2019; 513-521
- [27] Liu X, Jiang J, Zhang K, Localization and diagnosis framework for pediatric cataracts based on slit-lamp images using deep features of a convolutional neural network, *PloS one*. 2017; 12(3): e0168606.

- [28] Zhao W, Wang L, Zhang Z. Atom search optimization and its application to solve a hydrogeologic parameter estimation problem. *Knowledge-Based Systems*. 2019 Jan 1;163:283-304.
- [29] Burdziakowski P. Increasing the geometrical and interpretation quality of unmanned aerial vehicle photogrammetry products using super-resolution algorithms. *Remote Sensing*. 2020 Jan;12(5):810.